Fusion Engineering and Design 122 (2017) 288–298

Contents lists available at ScienceDirect

Fusion Engineering and Design

journal homepage: www.elsevier.com/locate/fusengdes

The DTT device: Rationale for the choice of the parameters

F. Crisanti[a,*], R. Albanese[b], R. Ambrosino[b], G. Calabro[a], B. Duval[c], G. Giruzzi[d], G. Granucci[e], G. Maddaluno[a], G. Ramogida[a], H. Reimerdes[c], R. Zagorski[f]

[a] ENEA-Frascati, Via E. Fermi 45, 00044 Frascati Italy
[b] ENEA-CREATE, Univ. Napoli Federico II, Via Claudio 21, 80125 Napoli, Italy
[c] Ecole Polytechnique Fédérale de Lausanne (EPFL), CRPP, CH-1015 Lausanne, Switzerland
[d] CEA, IRFM, F-13108 Saint-Paul-lez-Durance, France
[e] Istituto di Fisica del Plasma, ENEA-CNR Association, Milan, Italy
[f] Institute of Plasma Physics and Laser Microfusion, IPPLM Association, Warsaw, Poland

ARTICLE INFO

Article history:
Received 28 July 2016
Received in revised form 27 March 2017
Accepted 9 May 2017
Available online 30 May 2017

Keywords:
Power exhaust
Reactor relevant
Edge bulk integration

ABSTRACT

The main goal of the Divertor Tokamak Test facility (DTT) is to explore alternative power exhaust solutions for the next step after ITER, i.e., a demonstration power plant DEMO that will explore steady-state operation. The principal objective of DTT is to mitigate the risk of a difficult extrapolation to fusion reactor of the conventional divertor based on detached conditions under test on ITER. The task includes several issues, but with the main target to study the completely integrated (physics-technology and bulk-edge) power exhaust problems and to demonstrate how the possible implemented solutions (e.g., advanced divertor configurations or liquid metals) can be integrated in a DEMO device. This paper shows how the parameters for the design of a "flexible" facility, capable to perform this difficult task, can be worked out within the constraint of a fixed budget.

1. Introduction

As underlined within the European Fusion Road Map [1] power exhaust problem could be a possible "show stopper" along the route that leads to the achievement of an economic Fusion Power Plant (FPP). Among its numerous tasks ITER [2] will not be in the right position to face and completely solve such a problem (for instance it will be missing a metallic First Wall (FW) DEMO [3,4] relevant). Consequently, in the framework that there will be no further step between DEMO and the future Fusion Power Plant (FPP), the necessity springs out to have a facility able to study and solve the "integrated edge and plasma bulk" power exhaust problem: a Divertor Tokamak Test (DTT). Following the European Fusion Roadmap, the main objectives of the DTT device can be summarised as follows:

1) demonstrate a safe and robust power handling solution that can be extrapolated to DEMO;
2) achieve the previous goal without degrading the plasma core and pedestal performances, in a plasma regime as close as possible to a reactor one;
3) demonstrate the possibility to achieve points 1) and 2) by integrating as much as possible all the Physics and the Technological aspects.

The integration of these three targets is mandatory for meaningful experiments. It is a quite challenging task, since to simulate the complete behaviour of DEMO the only solution would be to realize DEMO itself. To overcome this very challenging issue, several different approaches have been proposed [5–7], either considering the divertor and the SOL as regions completely independent of the bulk plasma, or focusing the interest also on the core. In any case, a prioritization among the different parameters should be defined, trying to include all the different aspects as far as possible, compatibly with the available technology and economical resources. The main scope of this paper is to propose an approach, based on preserving the main physics aspect of the plasma edge and bulk, to design a scaled down facility capability to reproduce the conditions and issues to be faced to in DEMO, while maintaining some flexibility. It should be capable to explore at the best, from the physics and the engineering point of view, the largest part of the new ideas for solving the integrated edge-bulk power exhaust problem, i.e.,

* Corresponding author.
E-mail address: flavio.crisanti@enea.it (F. Crisanti).

http://dx.doi.org/10.1016/j.fusengdes.2017.05.053
0920-3796/

large radiation fraction, new divertor magnetic configurations, liquid metals and/or the integration of liquid metal with one of the new configurations.

In Section 2, the main parameters of the facility will be worked out by using an opportune 0-D scaling. In the Section 3, the performances of the facility are verified by considering an operational scenario and carrying out simple transport analyses. Section 4 is dedicated to the analysis of divertor and FW, to verify the correctness of the 0-D scaling. Since the facility will explore new magnetic configuration it is quite important to verify the possibility of the machine to withstand strong disruptions; this point is analyzed in Section 5, whereas Section 6 reports the main conclusions.

2. Rationale for the choice of DTT parameters

As underlined in the Introduction, any possible DTT facility must be finalized to study the integrated power exhaust problem. However, as well recognised in the literature [5], it is impossible to fully simulate a DEMO experiment with a smaller machine; consequently it comes out the necessity to introduce some prioritization in the DTT parameters choice.

Obviously, the first parameters to preserve are those connected with the divertor and the SOL regions. A key parameter characterizing these two regions is P_{SEP}/R [5], whose values should be around 15MW/m to be DEMO relevant (where P_{SEP} is the power flowing through the plasma boundary and R is the major radius). Other two important parameters [6] to be considered are the upstream poloidal (q_θ) and parallel ($q_{//}$) power fluxes: $q_\theta = P_{SEP}/\lambda_q 2\pi R$, where $\lambda_q \sim B_\theta{}^{-1}$ [7] is the decay length of the mid-plane heat channel. Since the parallel heat transport is dominant, it follows that $q_{//} \sim q_\theta B/B_\theta \sim P_{SEP}B/R$ (>110 MWT/m for DEMO [4]).

Previous works [8,9] have shown that, even considering the edge plasma as an insulated region, a complete "self-similarity scaled down experiment" cannot be realized, but that it could be approximated [10,8] by fitting five dimensionless parameters: T_e (normalized by a constant energy), $\upsilon^* = L_d/\lambda_{ei}$, Δ_d/λ_0, ρ_i/Δ_d, β, where L_d is the divertor field line length, λ_{ei} is the electron-ion collisional mean free path, Δ_d is the SOL thickness, λ_0 is the neutrals mean free path, ρ_i is the ion Larmor radius, β is the plasma pressure normalised to the magnetic one. Some of these parameters are intrinsically linked with the divertor magnetic topology and/or actual geometry; this fact immediately poses a first strong constraint for the DTT design: the necessity of having a very flexible divertor "region/configuration" to study and optimize the role played by the various topologically linked parameters. Eventually, the machine dimension and the plasma bulk performances should guarantee an exhaust solution extrapolating to a reactor-grade plasma. It is well known that the plasma physics properties (bulk and edge) are completely determined by the dimensionless parameters υ^* (normalized collisionality), ρ^* (normalized Larmor radius), β and T (dimensionless temperature, normalized to 1 KeV), [11,12]. However, as widely discussed in previous works [9], in a scaled down experiment it is not possible to preserve all these quantities simultaneously.

To come out from this impasse, a "weak scaling" strategy has been proposed, which consists in relaxing in a controlled way one of these parameters [13], so as to down-scale the main physics properties of a reactor-like experiment (i.e. ITER, DEMO) on a smaller experimental device, while preserving all the main physics aspects. Of course, the "best parameter" to "relax" depends from the main physics aspects that we want to preserve and study. In our, where we want to study the integrated aspects of the bulk and of the edge, clearly we cannot relax the temperature (that it leading all the edge atomic physics) neither the, since this would affect the local magnetic topology. Between υ^* and ρ^* we must consider that, again, υ^* depends strongly from the temperature and that, since $\rho^* \propto T^{0.5}/BR$, it is practically impossible to exactly preserve this parameter without using machine and plasma parameters requiring magnetic fields that are not technologically achievable (ρ^* = constant $\Rightarrow B \propto 1/R$). Consequently ρ^* is the dimensionless parameter that must/can be relaxed in the controlled way: $\rho^*_R = \rho^*_S R^\varepsilon$, the subscripts R and S indicate respectively the "reactor" and the "scaled" device, whereas ε is a controlled scaling parameter. In principle, a choice like this allows a 0-D scaling that preserves the main physics properties in a scaled experiment dedicated to study the power exhaust problem with a very flexible divertor region and significant values of P_{SEP}/R ($\geq$15 MW/m) and $P_{SEP}B/R$ ($\geq$110 MWT/m), and a set of dimensionless parameters as close as possible to DEMO. Of course, once the main machine parameters have been selected and a conceptual design worked out, a more detailed analysis has been performed to verify and to refine the assumptions.

When fixing the machine dimensions, on top of the technical and physical criteria already discussed, we must introduce another important constraint, i.e. the cost containment. It has to be underlined that of the cost parameter will act only as a problem constraint used only to fix the largest achievable machine dimension, but without affecting at all the scaling of the physics parameter. Only the fusion achievable performances (for instance the fusion energy gain factor Q) are strongly dependent on the size (and the cost) of the machine. The cost of a Tokamak (without using Tritium and not including the additional power) scales as the machine magnetic volume, cost$\propto B^2R^3$. When relaxing ρ^* by assuming $\varepsilon = 0.75$, we get cost$\propto B^2R^3 \propto R^{2.75}$ [13]. Of course this scaling leads only to a very rough preliminary evaluation of the machine actual cost that will has to be verified once the actual preliminary design will be realized; however its "solidity" can be easy verified [14] against the cost of existing machines and/or compared with the present cost of JT-60SA. As mentioned, the cost of the additional heating is not included in this scaling. To consider it, we can reasonably assume to be around one third of the maximum cost ratio between the whole machine and the total additional power: Heating_cost/Total_cost $\leq$ 0.3, e.g., Heating_cost $\approx$ 150M€ for a total machine cost of 500M€. Of course, in selecting this ratio, we introduce some "subjectivity" in the scaling, but this 0-D approach is only used to find out a "range" of possible machine sizes; once an actual dimension is fixed, everything will have to be verified within the actual performances and cost. This is mainly true for the additional heating, which strongly depends (physics, technology and cost) from the selected heating scheme. In Fig. 1, the value of P_{SEP}/R versus R is shown, as obtained by using the above-mentioned weak scaling, for three different values of the controlling parameter ε. It is immediately clear that by increasing ε above a certain limit there could be an intrinsic difficulty in achieving P_{SEP}/R values that are reactor relevant. On the other hand, for values of $\varepsilon = 0.5$ or less the additional heating would increase more than 1/R.

Consequently an intermediate $\varepsilon = 0.75$ value seems to be an appropriate scaling controlling parameter. When fixing an opportune ε value and a rough estimation of the machine cost (not including the heating) we can use the above-mentioned scaling to evaluate the cost of a proposed machine versus its major radius. This feature is shown in Fig. 1, which clearly shows that, to stay within a budget of about 350 M€, the maximum machine radius cannot exceed 2.3 m: $R_{Max} \leq$ 2.3m. Of course, the cost evaluation shown in Fig. 1 is only a very rough estimation and the actual machine cost has to be verified by a much more accurate analysis, once the machine design has been completed [15] So far we have just "fixed" (with a bit arbitrary criterion) a maximum budget for the additional heating, and, once fixed the maximum radius, a maximum necessary additional power, but we have not discuss

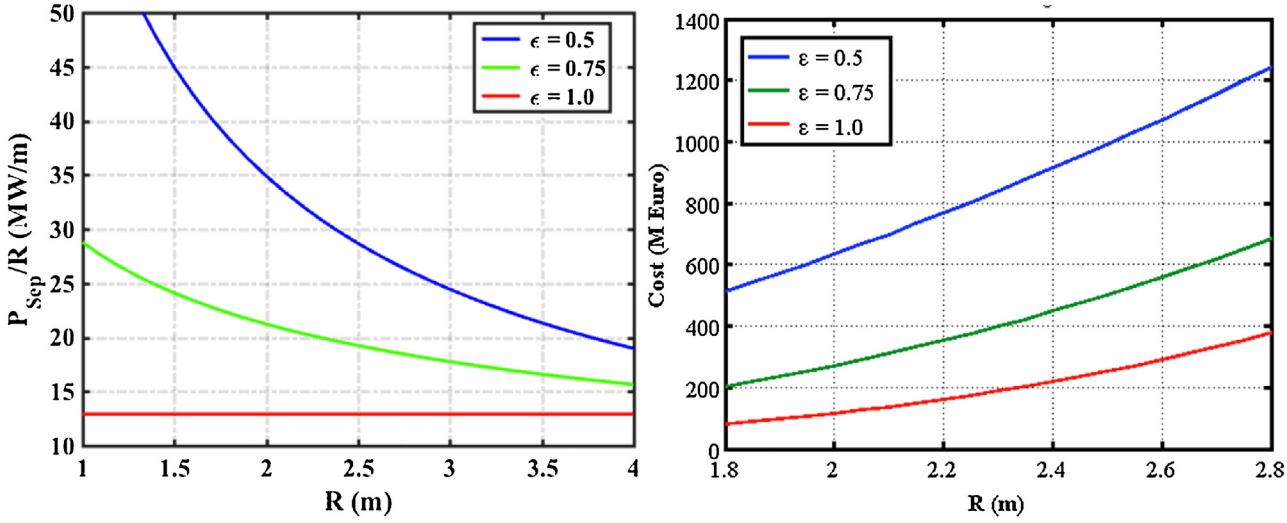

Fig. 1. P_{SEP}/R and cost scaling versus R for three different ε parameters. Left: P_{SEP}/R, which for $\varepsilon = 1$ is always too small. Right: Load assembling device cost, which for $\varepsilon = 0.5$ is always too high.

at all the compatibility between these two features. Only fixing a machine dimension, the P_{SEP}/R criterion will allow determining the minimum necessary additional power and the compatibility with the allocated budget. A meaningful minimum machine radius is not obtainable by the proposed physics scaling but a strong indication can be obtained from the first, and most important, introduced constraint of having a very flexible divertor region and actively cooled plasma facing components. This flexibility will be used (along the time machine life) to "easily" change different divertors, designed to best fit the different magnetic topologies and/or test different materials (tungsten, cooling pipes in copper alloys, liquid metals . . .). At the same time, this flexibility will also give the possibility to test different FW materials, and technologies in reactor relevant regimes from the point of view of plasma bulk performances and power flow.

In order to achieve such flexibility on plasma facing components and different magnetic divertor topologies and concepts (e.g., liquid metal divertor), a minimum machine radius is required. Again, the exact definition of this minimum radius will be a compromise among several different factors (including the total cost, which in some case could even increase when decreasing the size!) and a careful and quantitative analysis would require a detailed analysis of the proposed machine layout. Here we will only quote three arguments, which can already give significant indications about the quantification of a minimal machine dimension.

1) The machine target, to study quite different divertor magnetic topologies, makes it necessary to introduce a small set of internal coils (in our case four), to modify the reciprocal position of the main X point and of a second magnetic field null. Since $\lambda_q \sim B_\theta^{-1}$, in order to approach λ_q values similar to those of DEMO, the local field that has to be modulated is of the order of a few hundreds of gauss. Assuming some typical current density values ($30 \div 50\,MA/m^2$) the minimal dimension of each coil (including the mechanical support) is of the order of 10×10 cm, which implies, for the set of four coils, a radial extension of about $40 \div 50$ cm. With an aspect ratio of three we have a first rough indication that $R_{Min} > 1.5$ m.
2) In Fig. 2, the injected additional power, normalized to the plasma toroidal surface, is plotted versus the machine radius, assuming P_{SEP}/R = constant = 15MW/m. For comparison the power flux towards the FW for the present operating Tokamak AUG (see Table 1) is shown, together with the safe figure ($\approx 1\,MW/m^2$) for a reasonable power flux on a tungsten FW. It appears that by reducing too much the machine size ($R < 1.5$ m), the power density flux increases above the material safety limit. Even considering that approximately only 50% of the power interacts with the FW, a peaking factor of around $2 \div 3$ should be taken into account; therefore, the assumed power flux is still valid.
3) The third and last example regards the discharge duration time (τ_S) (to be discussed in more details in the next sections together with the connected technology). Here we just assume that the discharge must last longer than any thermalization time, and check how this assumption is affected by the machine size. Fig. 2 shows how the discharge duration depends on the plasma major radius, by using a standard scaling [16] and at fixed B_T, q_{95} and aspect ratio; the parameter "b" is the distance between the inner edge plasma radius and the outer radius of the central solenoid. For a given toroidal field and aspect ratio, this distance is roughly fixed, regardless of the used coils technology, copper or superconductors. In the case of copper, reducing "b" would mean to increase the current density in the toroidal magnet, up to a level where the discharge duration is not any more determined by the available flux, but by the magnet coil heating. For instance in our case, with $B_T \approx 6$T and by imposing a current density around $70\,MA/m^2$, the total distance "b" would be around 50 cm and the magnet heating would impose $\tau_S \approx 60 \div 70$s. By using superconductors we would not be limited by the coil heating, but the averaged current density should be smaller and the coils must be shielded against the neutron flux. Consequently, even by using superconductors we get $b \approx 50 \div 60$ cm. As well as for the other examples it appears that the machine size cannot be reduced below a certain level.

From the overlap of these three lines of reasoning we can roughly estimate a minimum value of the major radius. The first two arguments are the ones mainly related to the machine flexibility. Since both of them suggest a minimum plasma radius larger of 1.5 m, to stress the facility flexibility, the final chosen plasma dimension has be much larger than 1.5 m, therefore $R_{Min} = 1.7 \div 1.8$ m.

The upper bound for the major radius is mainly dictated by the budget limit. Remaining with the assumption of 1/3 of the total cost for the heating, from Fig. 1 it is immediately clear that a machine of the JET size ($R \approx 3$ m) without tritium would cost around €1 billion. Of course, a budget of this extent might also be used to

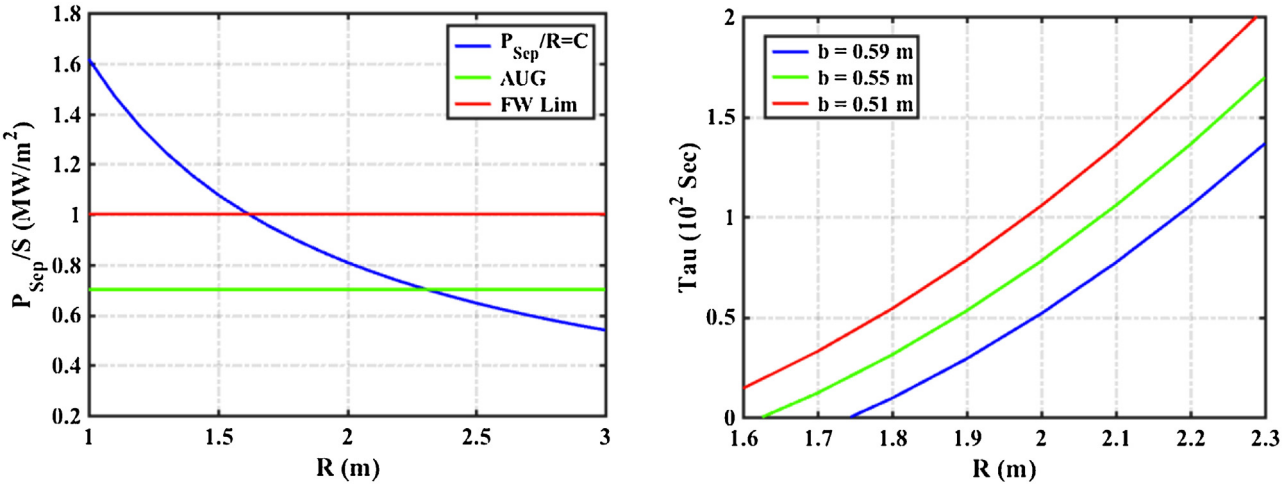

Fig. 2. Power density and pulse duration. Left: First wall power density versus the machine radius, assuming P_{SEP}/R = constant = 15MW/m. Right: Discharge duration versus the machine radius, with different values of the central solenoid width (b is the distance between the inner edge plasma radius and the outer radius of the central solenoid).

Table 1
Machine comparison.

	JET	AUG	EAST	DIII-D	ITER	DEMO(*)	JT-60SA	WEST	TCV	ADX	DTT
R (m)	2.98	1.65	1.7	1.67	6.2	9.1	3.0	2.5	0.88	0.73	2.15
a(m)	0.94	0.5	0.4	0.67	2.0	2.93	1.2	0.5	0.24	0.2	0.70
I_p (MA)	3.5	1.6	1.4	2.0	15	19.6	5.5	1	0.45	1.5	6.0
B_T (T)	3.2	2.4	3.4	2.1	5.3	5.7	2.3	3.7	1.45	6.5	6.0
V_p (m^3)	82	13	10	19	853	2400	141	15	1.85	0.9	33
($10^{20} m^{-3}$)	0.9	0.9	1.0	0.85	1.0	0.9	0.9	0.8	1.2	4.5	1.72
$/n_G$	0.7	0.5	0.4	0.65	0.85	1.2	0.8	0.7	0.5	0.4	0.45
P_{Tot} (MW)	30	25	30	27	120	460	41	16	4.5	14	45
τ_E (s) (H_{98} = 1)	0.49	0.07	0.07	0.11	3.6	4.2*	0.62	0.05	0.027	0.05	0.47
(KeV)	3.3	2.5	3.3	2.8	8.5	13.1	3.4	2	0.8	1.7	6.2
β_N	1.8	2.4	2.2	2.9	1.6	2.25	2.4	2	2.7	2.2	1.5
β (%)	2	2.8	2.3	3.6	2.2	2.6	4.5	1	3.5	2.0	1.8
υ^* (10^{-2})	8.6	8.4	7.4	4.0	2.3	1.4	4.1	35	65	13.1	2.4
ρ^* (10^{-3})	4.0	8.5	8.5	7.2	2.0	1.5	4.5	5.0	17	7.7	3.7
T_{Ped} (KeV)	1.7	1.3	1.7	1.4	4.3	5.5	1.7	0.5	400	1.3	3.1
n_{Ped} ($10^{20} m^{-3}$)	0.7	0.7	0.9	0.7	0.8	0.6	0.7	0.5	0.9	3.8	1.4
υ^*_{Ped} (10^{-2})	22.6	22	21	10	6.2	4.5	11	92	170	35	6.3
ELMs En. (MJ)	0.45	0.06	0.07	0.13	24	85	1.1	0.2	0.03	0.02	1.2
L-H Pow. (MW)	9.5 ÷ 12	3 ÷ 4	3.5 ÷ 4.5	3.0 ÷ 4.0	60 ÷ 100	120 ÷ 200	10 ÷ 12	4 ÷ 6	0.6 ÷ 0.8	4 ÷ 6	16 ÷ 22
P_{Sep} (MW)	21	18	21	18	87	150	29	10	3	9.5	32
P_{Sep}/R (MW/m)	7	11	12	11	14	17	9.5	4	3.4	13	15
λ_{int} (mm)	3.2	3.7	2.6	3.6	2.2	2.2	3.7	3	5.5	1.7	1.7
P_{Div} (MW/m^2) (no Rad)	28	44	62	45	55	84	24	25	7.3	110	54
P_{Div} (MW/m^2) (70% Rad)	8.6	13	19	13	27	42	7.4	7.5	2.2	33	27
$q_{//} \approx P_{Tot}B/R$ (MWT/m)	32	44	60	40	100	290	22	23	5	125	125
Pulse Length (s)	≈20	≈6	??	≈ 6	400	7600	100	1000	5	3	100

(*) For DEMO [iv] H = 1.1.

have a machine including tritium operation without increasing the dimension.

3. Plasma performance and operational limits

In the previous section, the use of a weak Kadomtsev like scaling and a reasonable use of the flexibility constraint has allowed to fix a minimum and a maximum meaningful plasma radius ($1.7m \leq R \leq 2.4$ m), when accounting all the most important physics constraints together with the budget availability. Within this range, we can then select a specific value of the major radius and check (on the basis of a draft design) the performances and the cost of the machine, by using appropriate and more sophisticated tools. Of course, only at the end of this exercise we will have the possibility to reconsider the machine parameters to accomplish at the best with the DTT mission and the budget cost.

Having in mind that the machine flexibility, in varying as much as possible the local divertor magnetic topologies, different divertor geometries, and/or different materials (including liquid metals), will strongly depends from the chosen machine size (R_{MIN} » 1.5 m), from Fig. 2, a reasonable choice for the machine dimension can be assumed to be R = 2.15 m. Of course, eventually this choice have to be verified by more sophisticated tools, as discussed in the related papers of this Special Issue on DTT. In order to finalize the machine size the machine aspect ratio A = R/a remains to be fixed. Presently the European DEMO [17] is studying different options with 2.7 < A < 3.5, consequently it seems a reasonable choice to propose a DTT with A ≈ 3. The use of the "weak scaling" allows to select the toroidal field (B_T = 6T) and the plasma current (I_P = 6MA) necessary to preserve (assuming an H_{98} = 1 confinement time) the important dimensionless parameters. In order to have $P_{SEP}/R \approx 15$, accounting for some bulk plasma radiation, a total additional power $P_T \approx 40 \div 45$ MW is needed. It has to be underlined that being DTT

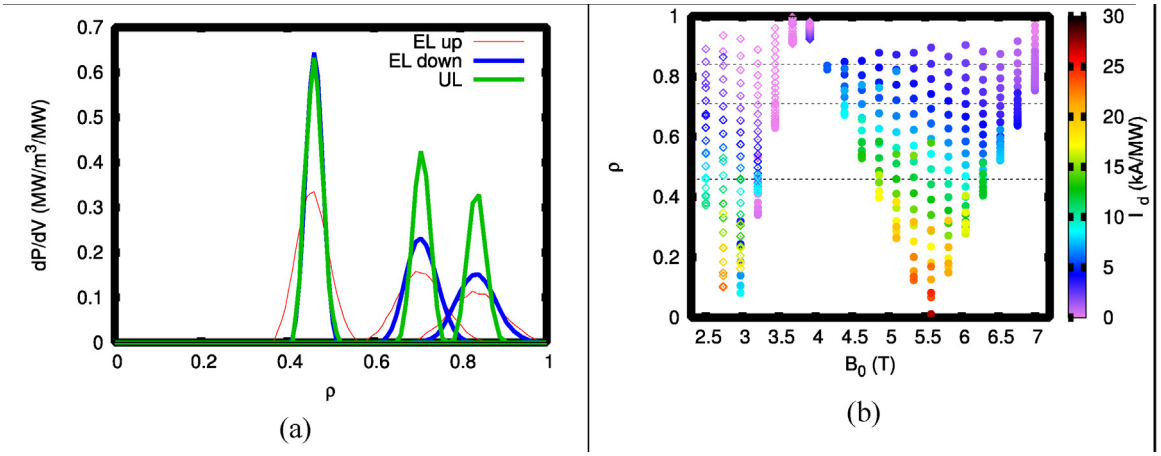

Fig. 3. Power deposition: (a) Absorbed power density dP/dV for injection from the equatorial (EL) and upper (UL) port, aiming at the q = 1, q = 3/2, and q = 2 surfaces with a toroidal launching angle β = 10° (for the equatorial launcher both upwards and downwards injections have been considered, reaching the rational surfaces above and below the equatorial plane, respectively); (b) Radial locations ρ that can be reached (vertical axis) at different magnetic field strengths B0, via a poloidal steering of the beam for a toroidal injection angle β = 16° (the corresponding driven current I_{cd} is indicated by the color code); injection of both O-mode (full circles) and X-mode (open diamonds) is considered.

a facility dedicated to the power exhaust, no particular attention has to be taken on the selection of a particular heating scheme and, in particular, no major attention has to be put on the current drive problems.

Since it would be even unthinkable to be able to couple all the target additional power from the very first operation day, it has been planned to realize all the necessary support facilities, but actually to bring in the additional power along the machine experimental life [15]. During the machine start up phase 25 MW (where we quote the power actually coupled with plasma) will be already available: 15 MW from ICRH (tunable between 60 and 90 MHz, with 32 ÷ 21 MW available from the generators) + 10 MW from ECRH (170 GHz). In a second phase additional 10 MW from ECRH will be installed. In a third phase the additional power will achieve the target of 45 MW by adding extra 15 MW to be chosen between ECRH and an NNBI system at 300 KeV [14]. It has to be noted that in the proposed reference scenario (with 15 MW coupled to the plasma), ICRH is assumed to work in H minority at the highest 90 MHz frequency, where the tetrode efficiency is the lowest. Choosing to use the ICRH in an heating scenario with ^{3}He minority, the tetrode efficiency upgrades strongly, up to about 25 MW coupled to the plasma. This possibility increases the total heating system flexibility, and in particular guarantees large margins for getting a robust H mode along the first operational phase. All the systems and the related physics are described in [15]. However, since ECRH is the main system, it is worth to shortly quote here its main features. The wave absorption and driven current with O-mode injection at 170 GHz have been evaluated with the beam-tracing code GRAY [18] for the reference plasma scenario with the two types of launcher, upper or equatorial. The typical power deposition widths are illustrated by Fig. 3a The profiles are broader for the Equatorial Launchers (EL) than for the Upper Launcher (UL), due to the longer path experienced by the beam, and to a worse "alignment" among beam trajectory, resonance and flux surfaces, especially when aiming above the equatorial plane. The current I_{cd} driven from the upper port at mid radius ρ = 0.5 is maximized with a toroidal injection angle $20° \le \beta \le 24°$, while for the equatorial port I_{cd} is maximized at $24° \le \beta \le 28°$. Using the upper launcher, with β = 16° current can be driven in the range $0.3 \le \rho \le 0.9$, with an efficiency at the q = 1, q = 3/2 and q = 2 surfaces of the order of I_{cd} = 9 kA/MW, I_{cd} = 3.7 kA/MW and I_{cd} = 2.2 kA/MW, respectively. The maximum current that can be driven in the core at ρ = 0.3 from the equatorial launcher is I_{cd} = 16bkA/MW. A rough estimate of the efficiency of the EC system for a magnetic field strength different from the nominal value B_0 = 6 T has been obtained by rescaling the reference plasma scenario, keeping the edge safety factor and the Greenwald density fraction constant, i.e. altering B_0, I_p, n_e and T_e by the same scaling factor, in order to test magnetic field values in the range $2.5\,T \le B_0 \le 7\,T$. Fig. 3b shows the results obtained for the upper port. First results of NTM stabilization for the 2/1 and 3/2 modes have been obtained considering wave injection from the Upper Port and are reported in [15]. The L-H power threshold for a large set of different scaling of this quantity is quoted in Table 1. Since the first day of operation the available power coupled to the plasma will be a factor of 1.1 ÷ 1.6 larger of any of these threshold, if we assume the most used L-H scaling ($P_{L\text{-}H} = 0.049\, n_e^{0.72}\, B_T^{0.80}\, S^{0.94}$, where S is the toroidal surface), we get $P_{L\text{-}H}$ = 18.5 MW, i.e. $P_{ADD} = 1.35 P_{L\text{-}H}$.

Having fixed the machine major plasma radius, the aspect ratio and the total additional heating, the use of a system code tool will allow an estimate of the machine performances and comparing them with other devices (existing, under construction or proposed, see Table 1).

Table 1 shows values of density and Greenwald fraction for various machines. An "operational" density has been chosen, that scales with respect to the ITER and DEMO ones as the other machine parameters. The maximum available or planned additional power P_{TOT} has been quoted for all the machines. For the power flowing through the last magnetic surface, P_{SEP}, there is always a large degree of uncertainties, depending on the bulk radiation fraction that, in turn, depends on the assumed experimental scenario. The quoted λ_{int} is the power decay length, by assuming Eich scaling [7], and where the smallest possible value has been assumed for the width of the flux in private region, consequently the quoted fluxes are describing a slightly "pessimistic" case. For a "fair" comparison in Table 1, 30% of bulk plasma radiated power has been assumed for all the machines, except for DEMO [4] (where a reference 60% is quoted). In the DTT the very high density (even at low Greenwald fraction) gives the very important advantage/flexibility, to be able to work in very high radiation regimes and study the interplay between advanced divertor configurations and the radiation in the various zones (bulk, SOL, divertor). The study and the optimization of the interplay between the radiation and the divertor magnetic geometry is the main target of the DTT proposal, consequently these aspect is extensively discussed in a dedicated paper of this Special Issue [15]. It is very important to note that only DTT

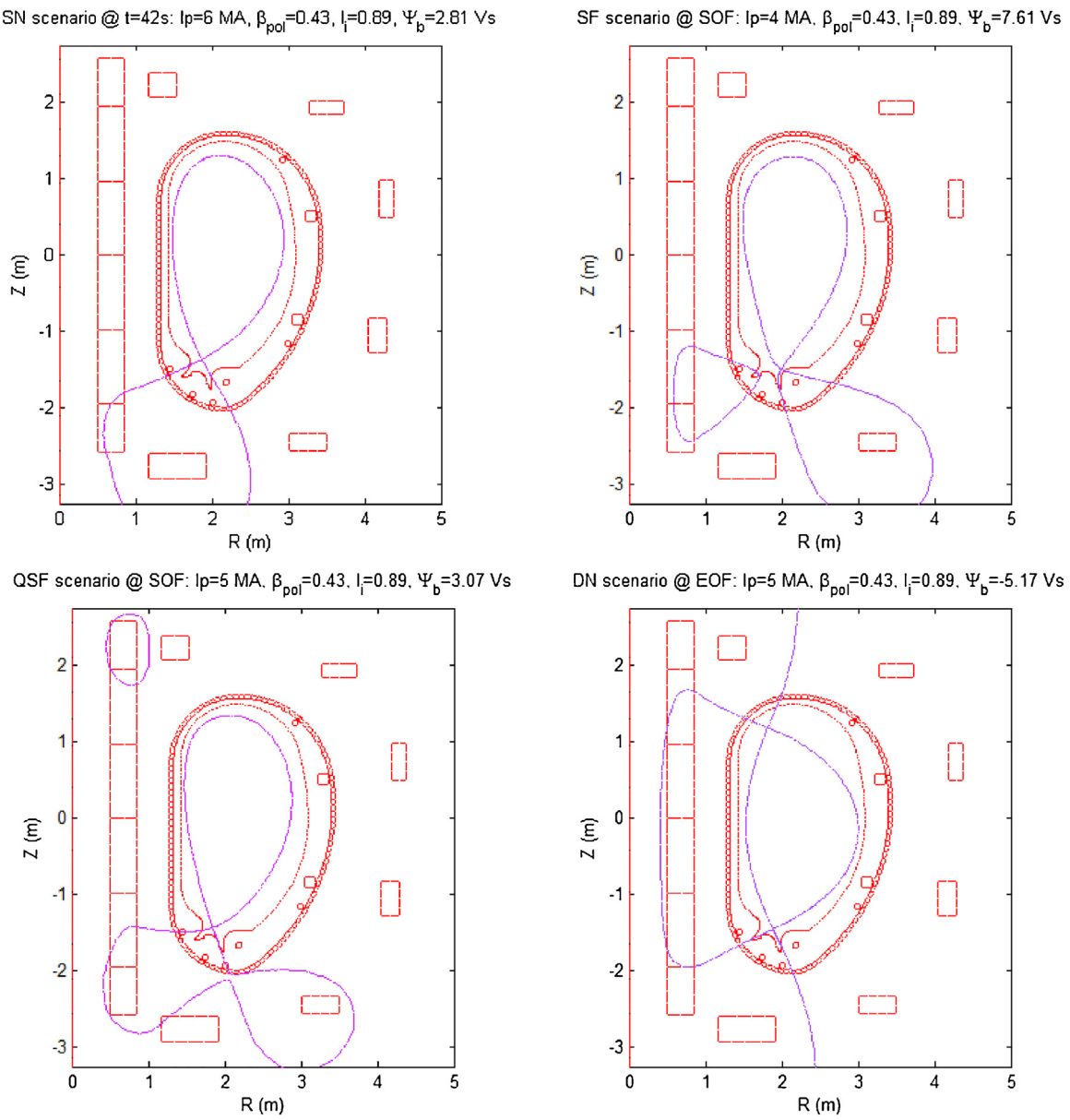

Fig. 4. Four different DTT possible equilibria: Top left – standard SN configuration. Top right – pure SF. Bottom left – QSF configuration. Bottom right – Double null.

and the proposed ADX tokamak [6] have a parallel heating flux feature comparable to a reactor one. All the dimensionless parameters defined in the previous section (averaged in the bulk region and/or in the edge) are very close to the ITER and DEMO [4] ones. As requested by our initial specifications, this will allow to correctly studying the SOL and divertor physics in reactor relevant regimes and, at the same time, with the necessary integration with a bulk plasma as close as possible to the DEMO one.

The duration of the discharge τ_S has to be determined taking into account all the characteristic times of the experiment. From the bulk plasma point of view τ_S has to be much longer than τ_{Res} (∼10s), being this the current density diffusion time (the longest physics characteristic time). From the divertor and FW point of view the discharge must last more than any thermalization time (τ_T); this will depend on the materials, but it is always longer than τ_{Res}. The exact definition of a characteristic thermalization time is not straightforward, but the ordering $\tau_{Res} < \tau_T < \tau_{FT\_MIN}$ easily allows a very minimal flat top time duration as $\tau_{FT_MIN} > 50$s. Considering a few tens of seconds (≈30 s) to build up the configuration and to get a steady plasma flat top, there will be about 70 s to study the integrated scenario. By assuming 30 s (3 τ_{Res}) to have a steady bulk, it will remain something around 40 s for any thermalization process that should be more than enough for studying the different divertors (geometry, material, magnetic configuration) properties. The use of superconducting coils [15] will allow plasma scenarios [15] lasting more than 100 s, assuming no external current drive and being limited by the stored flux.

The DTT flexibility in varying the local divertor magnetic topology has been verified and is discussed in a dedicated paper within this Special Issue [15]. In Fig. 4 the possibility to study a wide spectrum of local magnetic configurations is illustrated: the standard Single Null (SN), the Snow Flake (SF), the expanded boundary (XD) and the double null (DN). For any of this configuration a complete plasma scenario has been studied, verifying the compatibility with all the operational constraints (coils currents, coil forces, vertical stability, discharge duration, . . .). Moreover, for any of them a safe figure of around 10% has been used to remain within the actual limit operational limits. The complete interconnection of all these

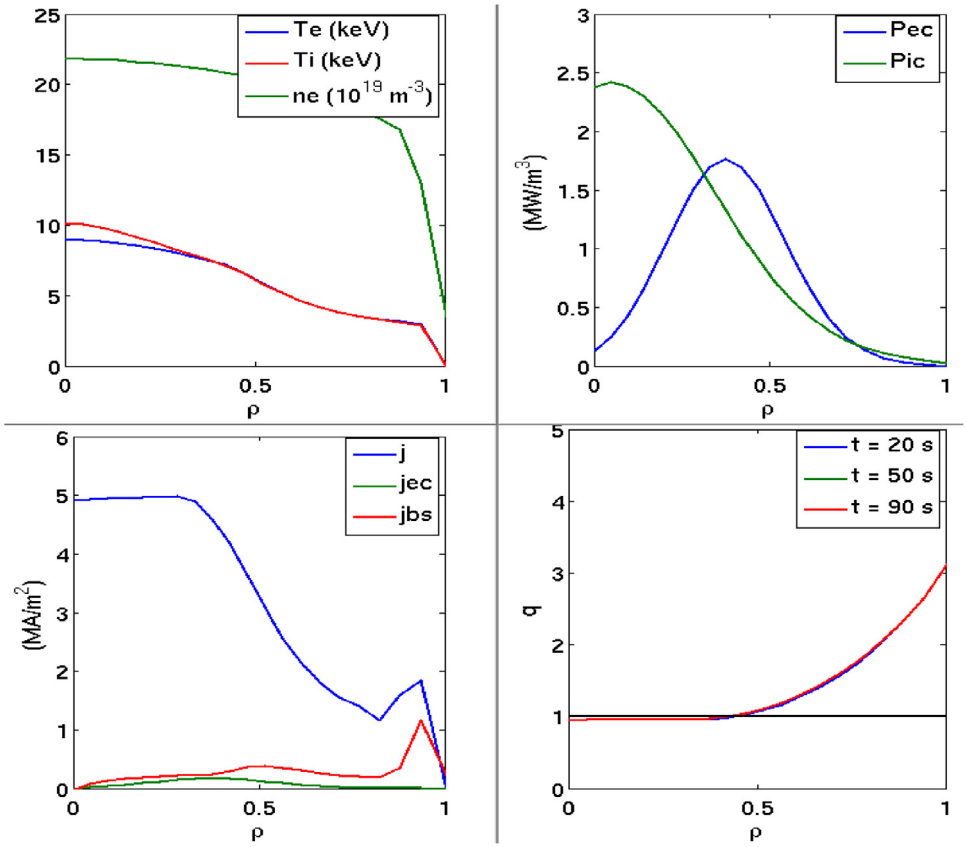

Fig. 5. METIS simulation –Top Left: density and Te, Ti profiles; Top Right 20 MW ECRH + 20 MW ICRH absorption profiles; Bottom left current density profile; bottom right q profile.

limits, sometimes is limiting the actual achievable plasma current for some configuration (see Fig. 4). However, the main limitation comes from connecting the equilibrium with the flux consumption. Consequently, by reducing the pulse length, it will be possible to increase the achievable plasma current. A final optimization will be possible once the machine will be realised. A set of small internal coil will allow playing around with the reciprocal position of the two nulls, characterizing all the alternative configurations, in order to study the physics of these configurations at the best [19].

The use of the simplified integrated modelling code METIS [20] (hybrid 0D/1D heat transport approach plus a 2D equilibrium solver) and of the integrated EDGE-CORE code COREDIV [21] [15], has allowed a robust verification of the quantities reported in Table 1. In Fig. 5 we report a METIS simulation where 20 MW of electron cyclotron (170 GHz) and 20 MW of ion cyclotron (90 MHz) have been used. The global values, predicted by METIS, fit quite well the figures given by the 0-D analysis. The use of two different radiofrequency heating schemes allows a large flexibility in the power deposition (top right frame), from very centred up to half radius. Moreover, the use of ICRH and the very high working density guarantee a good balance between Te and Ti (top left frame). The current profile is monotonic and it is essentially driven by the external transformer, with a large zone (up to around half radius) with $q \sim 1$, i.e. with a strong sawtooth activity.

4. Materials and technologies

Several different "technological aspects must be verified to be compatible with the machine scientific targets and the performed design choices. A dedicated section of this Special Issue [15] will deeply illustrate the machine flexibility in testing quite different divertor geometry (even optimized for a given magnetic configuration) and in testing quite different divertor materials. The basic option will consist in using the same technologies used for the ITER divertor and already working on EAST [22,23], namely tungsten monoblock actively cooled by water flowing in CuCrZr pipes. A thermo-hydraulic analysis (performed under the assumption of a power of around 20MW/m^2) with this divertor concept, carried out using pressurized water (4 MPa) flowing in the CuCrZr pipes at around 20 m/s, with an inlet temperature of 100 °C, shows that the surface temperature will never get higher than 1100 °C and the interlayer copper tungsten will remain around 400 °C. We already know that this pipe technology will not be suitable for DEMO [24,25], consequently different pipes realized with different materials (tungsten alloys) will be tested. The possibility of installing quite different divertor technologies, based on liquid metals [26], has been verified, even including a divertor realized with a 'separate' pool of liquid metal [27,28]. A preliminary fluid dynamic analysis of this divertor concept, based on the actual DTT geometry and technology, has been worked out [29]. The position of the outboard part of the Vacuum Vessel (VV) and the relative position of the FW are important items that impact on quite different aspects of the machine operations: plasma wall interaction, heating scheme, remote handling, material technology, etc. An analysis of these elements has resulted in an assessment of the main machine requirements for the actual outboard of the VV and the relative position of the FW.

The minimum distance of the FW from the plasma boundary will be of 4 cm (about ten times the midplane energy decay length, see Table 1). The FW will be realized by finned tubes of stainless steel (SS) with the plasma facing surface protected by some ($2 \div 5$ mm) thick coating of tungsten (W) deposited by plasma spray

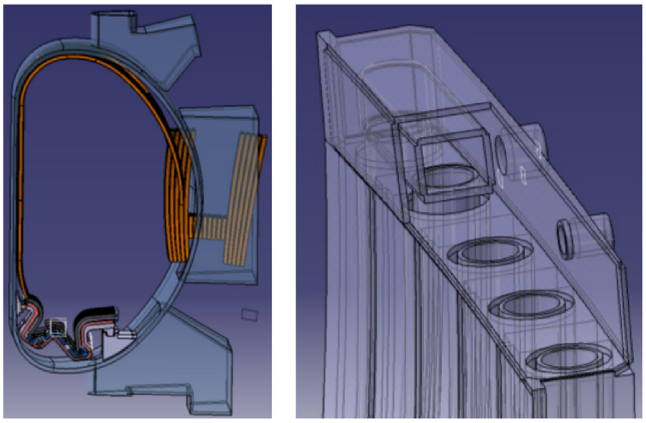

Fig. 6. Remote handling and design of the FW.

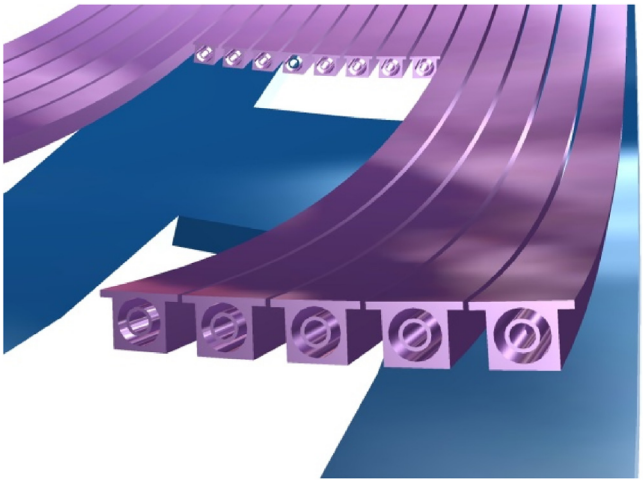

Fig. 7. Artistic view of the possible layout of the FW panels.

(see Figs. 6 and 7), capable to sustain up to around 5 MW/m^2 [30]. Assuming that DTT will radiate 100% of the power, the highest averaged FW wall power load will not exceed 0.5 MW/m^2, even assuming a peaking factor of the order $2 \div 3$, thus the highest average flux will remain well inside the proposed technology. During disruptions and the start-up phases (when the FW is operating as a limiter) larger power load can be experienced (up to $3 \div 4$ MW/m^2) on the inner midplane side and/or on the upper part, for this reason, on that region the W coating will be larger, of the order of 1 cm. The large coating thickness, suitable for the expected moderate heat loads, guarantees a long lifetime for components not easily removable and plasma spray is the most suitable and cheapest technique for coating deposition on large components. For getting around the problem of the mismatch between the thermal expansion coefficient of W and SS, a suitable interlayer will be deposited before the W coating. Functionally Graded Material (FGM), consisting only of a mixture of W and SS powder, will be preferentially used for the interlayer. Mock up of straight and curved finned SSl tubes coated with thick W deposit have been already realized and will be tested under high heat fluxes in relevant facilities like Judith and/or Gladis. Several different options are under activation for an active control of the FW temperature. In a first "traditional" option FW will be actively cooled by pressurized water with a velocity of 5 m/s with a temperature be kept at around 100 °C. However 100 °C will not be enough when working with a liquid metal divertor, consequently a second option foreseen the use of pressurized He to keep the FW temperature around $300 \div 400$ °C. Of course the two systems will not be compatible, consequently the final choice will be made once all the technical issues will analysed in detail, during the next DTT engineering phase. Presently the preferred option is to use the pressurized He FW temperature control, since this solution is much more robust, when working with liquid metals, and because an high FW operational temperature is foreseen for DEMO. The FW will be replaceable for maintenance reasons as well as for scientific reasons.

In steady state operations, during the inter-ELM phase, the contribution of charged particles to the power load on the FW is expected to be negligible, as the plasma-wall distance is everywhere much larger than the plasma power e-folding length. ELMs energy depends from the total energy stored in the plasma pedestal (at the maximum, in a good H, around 40% of the total volume averaged energy) and it is inversely proportional to the local collisionality [31]. Of course, the total stored energy is directly proportional to the plasma volume. Consequently, there is no possibility, on a scaled experiment, to have ELMs with energies comparable to the ones on a large volume reactor. However, since the DTT will have a pretty low local collisionality (in a high density regime, like in a reactor) and a meaningful ELMs energy ($\approx$1 MJ), this will allow to study ELM mitigation strategies in conditions relevant to DEMO. Presently the use of error field internal coils (with $n = 1 \div 2$) to moderate the ELM amplitude is under study; however, since this technique could not be used in DEMO, other strategies are under investigation (vertical kicks, pellets, local heating...), in order to achieve situation with lower ELM amplitude and higher frequency. As for the ELM phase, the turbulence driven filamentary transport of the plasma energy in the far SOL can lead to FW loads due to charged particles. Taking into account the poloidal extent of plasma filaments (about 10 cm for a plasma radius of 0.7 m [32]), the fraction of the ELM energy transported by a single filament ($\sim$2.5%, corresponding to $\sim$40 kJ in DTT), conservatively assuming no decay of the filament energy with the radial distance, with an ELM frequency of 10 Hz, we get for each filament at most about 400 kW deposited on a toroidal strip of $2\pi R_{omp}$ long and about 10 cm wide, yielding a load of 0.3 MW/m^2. The power transported by charge-exchange neutrals has to be better assessed, but it is not expected to be important. The main contribution to the FW load is instead by radiated power: by assuming that all the input power ($40 \div 45$ MW) is radiated in an isotropic way on the wall surface (about 90 m^2), the resulting average power density is around 0.5 MW/m^2. Even considering toroidal and poloidal peak factors of 3 the average heat load results in well tolerable values.

Another source of power load peaking on the FW is to be expected during the limiter phase of the discharge start-up, when the plasma-wall contact, although with input power limited to the ohmic fraction, is restricted to a reduced portion of the inboard FW. The need for the toroidal shaping of the sectors in the inboard wall, as done in the ITER design [33], has been examined.

5. Plasma disruptions

The DTT facility will be mainly devoted to explore new magnetic configurations, consequently a strong attention has to be put on the control aspects [15] and on the machine "robustness" against possible disruptive events. A very large power load by charged particles as well as larger radiation load peak factors are to be expected during transients like Vertical Displacement Events (VDE) and disruptions, together with large electromagnetic induced stresses on the material. Obviously this is an important question whose compatibility has to be verified with the machine chosen parameters.

According to Codes and Standards for ITER [34] and Design and Construction Rules for Mechanical Components of Nuclear Installations (RCC-MR) [35], the following four categories of event occurrence are defined:

I Operational (events intentionally triggered by the plant operator);
II Likely (events expected to occur up to about 100 times in the life of plant);
III Unlikely (events expected to occur less or once during the plant life);
IV Extremely unlikely (events with expected frequency of occurrence less than once every 10,000 years).

The following four criteria level can be also identified [34,35] to specify the damage level in consequence of an event for a given safety class:

A Negligible damage, all systems are functional.
B Negligible damage, all systems are functional but minor adjustments might be required.
C Possible significant local distortion.
D Possible large general distortion and investment loss.

A general rule states that criteria level A should be applied to events in category I and II, criteria level C to category III and criteria level D to category IV.

Suitable strategies will be put in place to reduce the risk of plasma disruptions, by designing safe operation scenarios with density and safety factor within the limits. However, when operating at high plasma current as in DTT, an additional risk to have a sudden disruption event arises, related to an increase of interaction among MHD modes [36]. This class of disruptions can be observed when the plasma inductance is relatively high for a given safety factor and causes high forces on the machine, due to the high currents involved [36].That should be considered in defining the probability of occurrence of the different disruption events. In elongated, high performance tokamak machines like DTT the EM loads produced by VDEs are by far the largest loads among those the VV must withstand and then will be used to assess its structural integrity. Two category IV event have been defined for DTT as upward or downward VDEs occurring at the end of the flat top, with the maximum plasma current and thermal energy, and evolving to the largest possible plasma vertical displacement without thermal losses until the safety factor at 95% flux surface goes below 1.5, when the thermal quench (TQ) and the fast current quanch (CQ) arise. This event is the worst expected accidental event for the DTT vacuum vessel (VV) integrity, due to the large vertical and horizontal EM loads produced by the vertically and toroidally asymmetric eddy and halo currents. This event has been modelled with both MAXFEA [37] and Carma0NL [38] codes. In these simulations the plasma is initially displaced by a sudden current "kick" by one of the poloidal field coil and then is left free to evolve, slowly moving upward or downward in the VV and shrinking in volume.

The plasma is partially stabilized in its movement by the eddy currents induced on the plasma chamber, with a characteristic vertical instability growth time, about 20 ms in DTT for a 50 mm thick SS VV. While the plasma column moves and shrinks, the safety factor drops off and the plasma current slowly decreases due to the poloidal flux conservation. During its movement the plasma interact with the FW or other in-vessel components, resulting in the cooling of the plasma edge and providing a path for the poloidal current to flow from plasma into the vessel and then again to the plasma on open field lines which are in thermal contact with the wall. In this phase some unstable modes can arise destabilizing the plasma and resulting in a sudden loss of its thermal energy, the TQ. The chance of arising unstable modes increases dramatically as the safety factor at the edge decreases, and the severity of the EM loads during a VDE largely depends on the value of the safety factor at the TQ, that is directly related to the vertical asymmetry of the induced currents on the vessel and then to the vertical forces applied to the VV. The occurrence of unstable modes is unavoidable when the safety factor at the edge goes below 2, so this event has been chosen as worst possible EM accident for the VV integrity and assigned to category IV faults, due to its fast (few ms) transfer to the chamber of the whole plasma thermal and magnetic energy with the largest vertical and possibly toroidal asymmetry. In DTT the minimum CQ duration (from 80% to 20% of the initial plasma current) with this scaling is 4.7 ms. Fig. 8 shows the time evolution of the main plasma macroscopic parameters during the Category IV upward VDE as modelled in MAXFEA. The induced (eddy and halo) current during the different plasma disruptions and the EM loads on the VV have been evaluated using MAXFEA and Carma0NL and will be used as input for the structural assessment of the machine in the next phase of the design. Carma0NL simulation results were recently compared with experimental data from EAST [39] and with MAXFEA simulations [40]. Fig. 8 shows the vertical forces on the VV due to the halo and eddy current in the worst case, i.e. during the Category IV upward VDE, as evaluated by MAXFEA. The maximum net vertical force on the VV reaches in DTT a value below 5 MN, as confirmed by first MAXFEA simulations in Fig. 9 and also as confirmed by a simple scaling with plasma current, toroidal field and minor radius [41]. With this value and assuming a SS VV with 50 mm thickness, similar results are found for the estimation of the maximum stress on the chamber and then its integrity is guaranteed in the worst accidental event. The maximum EM loads expected to be produced on the divertor during downward VDE, even if strongly dependent on the divertor design, are supposed, using similar extrapolation [41] to be slightly lower than in the FAST reference scenario. As for the thermal load on the FW, one of the worst scenarios is the thermal quench (TQ) occurring at the end of a VDE, with large part of the discharge energy content being suddenly deposited on the inboard FW.

A method for evaluating the potential damage of FW by disruption is to compare the calculated heat load with the so called damage parameter. The latter, from the surface temperature increase in the semi-infinite solid approximation (appropriate, given the very short energy load during the TQ) can be expressed as $D \approx W_{th}/(A_{TQ}\, t_{TQ}{}^{1/2})$, where W_{th} is the plasma thermal energy at the disruption onset, A_{TQ} the heat deposition area, and t_{TQ} the TQ duration. A value of $D \approx 40$–$60\ MJ\ m^{-2}\ s^{-1/2}$ corresponds to W melting. From past and present experiments t_{TQ} results to be approximately proportional to minor radius, although there is a large scatter of the data. For DTT t_{TQ} is very short, about 200 300 μs. The temporal behavior of the TQ transient loads on the PFCs is also important because it determines the expected material erosion for the given power fluxes. Indeed the above estimation of the TQ duration refers to the power rise time. Similarly to the ELM case it is found that a large amount of energy reaches the PFCs after the peak of the power flux. The decay phase of the thermal quench power pulse is typically a factor of 2–3 longer than the rise time. Thus, only ~30% of the total energy flux during the TQ reaches the target within the rise time phase. For the sake of simplicity we assume a total t_{TQ} of 1 ms. The heat deposition area can be calculated by taking into account that a broadening of the SOL width, with respect to the values of steady state, is usually observed during thermal quench for both divertor and limiter machines. Recent IR measurements on JET point out a broadening factor of about 4 for VDE. By assuming λ_q steady state ~1 mm the thermal energy at the disruption onset is considered to be deposited on a toroidal strip of $2\pi R_{imp} \times 0.025\ m = 0.23\ m^2$, where R_{imp} is the major radius of the inboard wall. As for the discharge thermal energy content just before the TQ, for several kinds of disruption this is lower, even much lower, of the thermal energy content at steady state, due to the pre-TQ confinement degradation this is not the case, for example, of Internal Transport Barrier (ITB) disruption. As first approximation let us assume that at the TQ the thermal energy

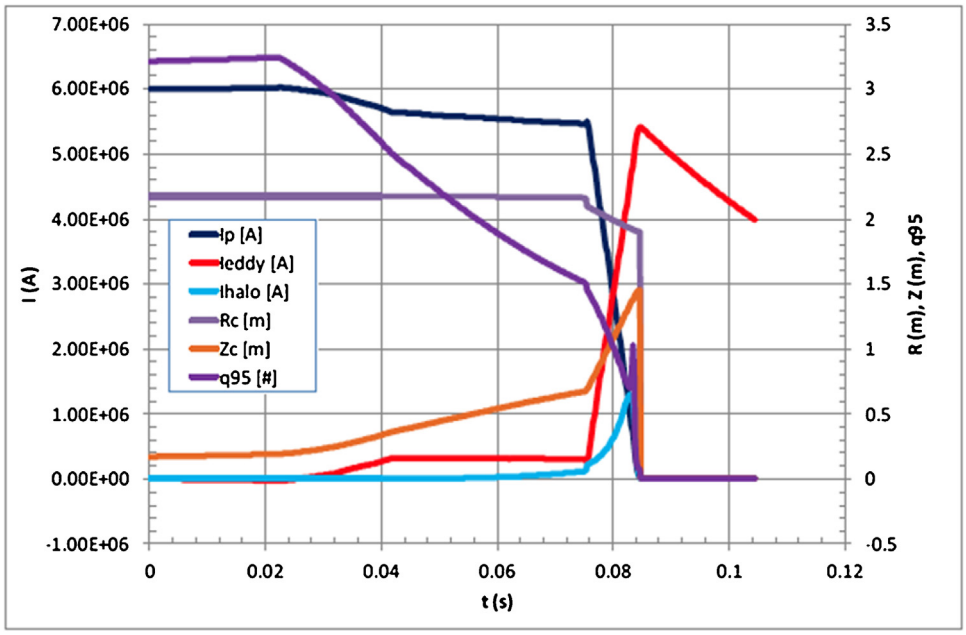

Fig. 8. Main macroscopic parameters evolution in the Category IV upward VDE by MAXFEA.

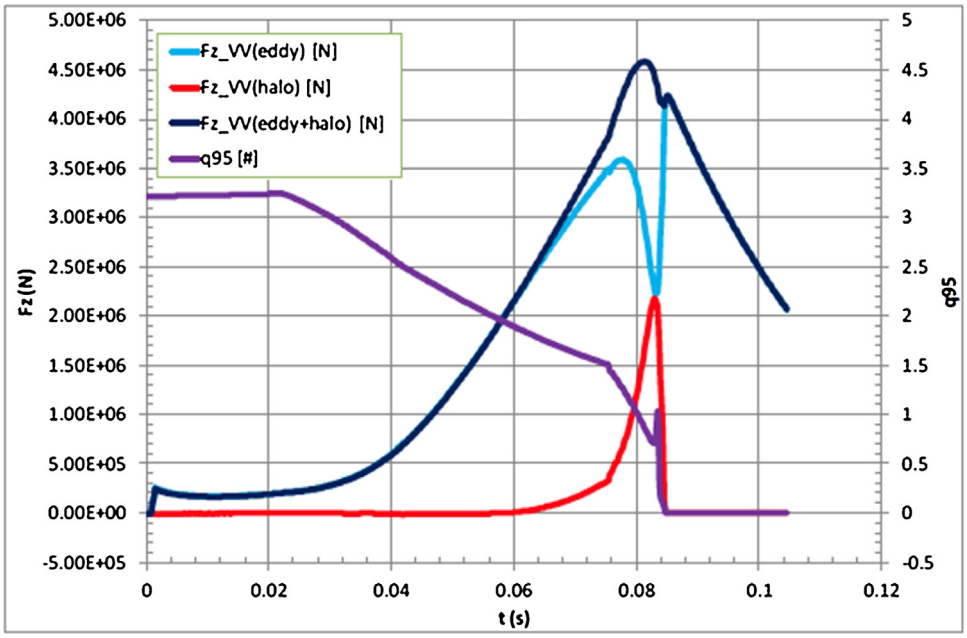

Fig. 9. Vertical forces on the VV due to the halo and eddy current in the Category IV upward VDE.

content is about 50% of the steady state content and that half of this energy is deposited by conduction-convection on the inboard wall, the other half being radiated mainly from impurities eroded from the wall during the TQ. Summarizing, the average heat load on the inboard FW of DTT during a VDE is about 190 MWm^{-2}. This very large value, although characterized by large uncertainties, which require further analyses, suggests that unmitigated disruption at high performance could lead to severe damage to the FW and that massive gas injection (MGI) technique is to be implemented. This also for the following argument, that is the specific concerns are given by the features emerging in the recent JET experiments with ITER Like Wall (ILW), characterizing the disruption events in a tungsten environment respect to a full carbon machine [42,43]. These experiments pointed out that the lack of a good radiating impurity like carbon results in a fraction of radiated power at disruption much smaller than before. In turn, this results in longer current quenches, larger heat loads caused by conduction of magnetic energy to Plasma Facing Components (PFC) and longer halo currents, producing larger impulses of the reaction force on the vessel and its supports. Temperatures above the melting limit of beryllium have been observed during VDEs in JET even with plasmas having relatively low current and thermal energy, because of the dissipation by conduction of the magnetic energy on relatively small areas along the magnetic field lines during the longest time typical of the ILW CQ. This fact led to the requirement in JET of using the Massive Gas Injection (MGI) to mitigate disruptions for plasma currents greater than 2 MA. A similar approach to the active mitigation of the thermal effects of the disruption events will be used

in DTT, exploring solutions with different kind and fluence of gas injected.

6. Conclusions

DTT is planned to be a facility entirely devoted to study the integrated bulk-edge power exhaust problem an to tackle the Physics and Technology divertor problems with sufficient flexibility to develop innovative divertor configurations bringing them to a sufficient level of maturity by 2030 for a positive and well assessed decision on DEMO [1]. Of course, when tackling a so challenging target there is never a single possible choice. In this particular proposal, the DTT device is conceived to be flexible enough to have the possibility to test both alternative magnetic configurations and advanced divertor technology, e.g. liquid metals, in DEMO relevant conditions, demonstrating an integrated exhaust scenario.

A key parameter, for a scaled experiment, is the ratio between the power across the separatrix and the major radius, which should be achieved for a safe DEMO operation, i.e.15 MW/m. In addition, to scale the divertor physics of a large machine five parameters should be fitted:

- the temperature, T_e
- the normalized local collisionality, $\nu_{div}{}^* = L_d/\lambda_{ei}$, where L_d is the divertor field length
- the neutrals free path, normalized to SOL thickness, λ_0/Δ_d
- the normalized Larmor radius, $\rho^* = \rho_i/\Delta_d$
- the normalized plasma pressure, β

Since most of these parameters depend on the magnetic divertor topology, this DTT proposal has been worked out to allow testing several different magnetic divertor topologies. By using a Kadomtsev-Lackner approach (based on preserving the dimensionless parameters ν^*, β, $\rho^* R^{0.75}$, Te) and taking into account a budget limit of 500 M€, a machine with a major radius of R = 2.15 m, a toroidal field B_T = 6T and a plasma current I_P = 6MA has been selected so as to guarantee the fulfillment of the DTT objectives. The coupled edge and bulk code COREDIV has been used to verify the expected edge performance, whereas the use of the simplified integrated modelling code METIS confirmed the expected bulk plasma performance.

The plasma scenarios (including standard single null and advanced configurations) will satisfy the following constraints:

- minimum distance of 40 mm between the plasma last closed surface and the first wall, in order to minimize the interaction between the plasma and the main chamber (the power decay length at 6 MA is ~2 mm);
- plasma shape parameters similar to the present design of DEMO [4]: R/a ≈ 3.1, k ≈ 1.6, <δ> ≈ 0.35;
- pulse length of more than 100 s with a total stored flux of about 45Vs.

The PF system is very flexible and will allow a large set of different divertor magnetic configuration: the standard SN, the snow flake, the expanded boundary and a double null. A set of small internal coils will allow locally "playing around" with any of these configurations in order to better understand the ruling physics and to select the best one for DEMO. The actual geometry of the VV is designed in order to accommodate a large set of different divertors, even including a divertor like an enclosed pool of liquid metal. A FW actively controlled in temperature (up to 300 ÷ 400 °C) and replaceable will be compatible with the possibility of testing different FW materials and the use of liquid metal in the divertor. As far as additional heating and current drive are concerned, the system for the first DTT phase includes 15 MW of ICRH and 10 MW of ECRH. NBI and ECRH are being considered as the main candidates for a subsequent power upgrade, up to the ultimate target of 45 MW.

References

[1] Fusion Electricity, A Roadmap to the Realization of Fusion Energy, 2012, November (http://users.euro-fusion.org/iterphysicswiki/images/9/9b/EFDA_Fusion_Roadmap_2M8JBG_v1_0.pdf).
[2] http://www.iter.org/.
[3] G. Federici, et al., Fusion Eng. Des. 89 (2014) 882.
[4] R. Wenninger, et al., Nucl. Fusion 57 (2017) 016011.
[5] K. Lackner, Com Plas, Phys. Control. Fusion 13 (1990) 163.
[6] D. LaBombard, Nucl. Fusion 55 (2015) 053020.
[7] T. Heich, Nucl. Fusion 53 (2013) 093031.
[8] D.G. Whyte, Fusion Eng. Des. 87 (2012) 234.
[9] K. Lackner, Com. Plas. Phys. Control. Fusion 15 (1994) 359.
[10] I.H. Hutchinson, Nucl. Fusion 36 (1996) 783.
[11] K. Lackner, Fusion Sci. Technol. 54 (2008) 989.
[12] B.B. Kadomtsev, Fiz Plazmy 1 (1975) 531.
[13] A. Pizzuto, Nucl. Fusion 50 (2010) 095005.
[14] http://fsnfusphy.frascati.enea.it/DTT/downloads/Report/DT_ProjectProposal_July2015.pdf
[15] Albanese A. Pizzuto, WPDTT2 Team, and DTT project proposal contributors, 'The DTT proposal. A tokamak facility to address exhaust challenges for DEMO: Introduction and executive summary' and related papers, 10.1016/j.fusengdes.2016.12.030.
[16] H. Zohm, Fusion Sci. Technol. 58 (2010) 613.
[17] R. Wenninger, et al., Nucl. Fusion 55 (2015) 063003.
[18] D. Farina, A quasi-optical beam-tracing code for electron cyclotron absorption and current drive: GRAY, Fusion Sci. Technol. 52 (2007) 154.
[19] F. Crisanti et al., DTT: an Integrated Bulk and Edge Plasma Experiment to Tackle the Power Exhaust Problem in View of DEMO, 26th IAEA, Kyoto, and Pericoli Ridolfini, et al. submitted to Nuclear Fusion.
[20] J.F. Artaud, et al., In 32nd EPS Conf. on Contr, Fusion and Plasma Phys., ECA Vol. 29C, P1.035 (2005).
[21] R. Stankiewicz, J. Nucl. Mater. 191 (337) (2005).
[22] R. Pitts, Physics basis and design of the ITER full-tungsten divertor, in: 55th Annual Meeting of APS Division of Plasma Physics, Denver, USA, 11–15 November 2013, 2017 https://www.burningplasma.org/resources/ref/1_Pitts.pdf.
[23] X.Y. Quian, et al., Nucl. Fusion 56 (2016) 026010.
[24] T.R. Barret, et al., Fusion Eng. Des 109 (2016) 917.
[25] J.W. Coenen, et al., Phys. Scr. TT67 (2016) 014002.
[26] L.G. Golubchikov, et al., J. Nucl. Mater. 233–237 (1996) 667–672.
[27] Y. Nagayama, Fus. Eng. Des. 84 (2009) 1380–1383.
[28] R. Goldston, et al., First IAEA technical meeting on divertor concepts, in: 29 September, 2 October, Vienna, 2015 (http://www-naweb.iaea.org/napc/physics/meetings/TM49934.html).
[29] R. Zanino et al., Modeling the Lithium Loop in a Liquid Metal Divertor for Future Fusion Reactors, 26th IAEA, Kyoto, and Zanino R. et al. submitted to Nuclear Fusion.
[30] M. Rödig, et al., Fusion Eng. Des. 56-57 (2001) 417–420.
[31] A. Loarte, et al., Progress in the ITER physics basis. chapter 4: power and particle control, Nucl. Fusion 47 (2007) S203.
[32] A. Kirk, et al., J. Phys.: Conf. Ser. 123 (2008) 012011.
[33] Horacek J. et al, 42nd EPS Conference on Plasma Physics (Lisbon, Jun 22nd −26th,2015).
[34] Codes and Standards for ITER Mechanical Components, v4.0, ITER_D_25EW4 K, 21/06/2012.
[35] Design and Construction Rules for Mechanical Components of Nuclear Installations, RCC-MR, French Association for the Design, Construction and Operating Supervision of the Equipment for Electro-Nuclear boilers (AFCEN), 2007.
[36] A. Vannucci, R.D. Gill, Nucl. Fusion 31 (1991) 1127.
[37] P. Barabaschi, The MAXFEA code, in: Plasma Cont. Techn. Meeting, Naka (Japan), 1993.
[38] F. Villone, et al., Plasma Phys. Control. Fusion 55 (2013) 095008.
[39] S.L. Chen, et al., Nucl. Fusion 55 (2015) 013010.
[40] F. Villone, et al., Fus. Eng. Des. 93 (2015) 57–68.
[41] B.N. Sorbom et al. ARC: A compact, high-field fusion nuclear science facility and demonstration power plant with demountable magnets, arXiv:1409.3540 2014.
[42] C. De VriesP, et al., Plasma Phys. Control. Fusion 54 (2012) 124032.
[43] M. Lehnen, et al., Nucl. Fusion 53 (2013) 093007.